

NUMERICAL INVESTIGATION OF THE EFFECT OF THE PERMEABILITY OF EAGLES AIRFOIL ON ITS AERODYNAMICS PERFORMANCE

Rania R. Rahuma¹ and Ashraf A. Omar ² and
Abdulhaq Emhemmed³
University of Tripoli
Tripoli, Libya

ABSTRACT

In this work, the findings of research conducted to determine the basic aerodynamic characteristics for 2D sections of the eagle airfoil where the permeability of the wings was simulated. Computational fluid dynamics (CFD) was used to determine the airfoils features utilizing the open source CFD code Stanford Unstructured (SU2). The simulated cases assumed incompressible, viscous and steady flow where the eagle assumed to be in gliding flight. The aerodynamic characteristics were evaluated for a range of angles of attack. In addition, a low Reynolds number man-made airfoil (Eppler 193) was also simulated for validation and comparison.

It was found that permeability increased the generated lift and efficiency for the eagle airfoil for angle of attacks smaller than 10°. The increase reached 58% at zero angle of attack. After the specified angle, permeability had adverse effects on the flow which maybe due to the transition to turbulence ahead of the permeable section. Finally, an overall consideration of the results indicated that the eagle's airfoil is more efficient than the man-made airfoil (E193).

INTRODUCTION

Birds are a wonder of nature, their flight mechanism reach a level of perfection in all aspects. These flight features are of considerable interest to biologists and engineers and they remain poorly understood. Birds, bats, and insects are able to generate relatively large forces very quickly in response to gust and other disturbances during different maneuvers. However, more detailed investigations are needed in this field to improve the general understanding of the flight features mechanisms. The nature of birds flight can be attributed and considered as the basic tool to aeronautical systems. The nature of birds' flight can be attributed and considered as an important tool to the development of aerodynamics and aeronautical systems in general. They are especially important in the aerodynamics of micro aerial vehicles (MAV) and low Reynolds number flows. A bird wing porosity leads to a significant difference in the air transitivity between inner and outer feather vanes. This was studied by a few researchers to obtain general understanding of the flow of air when it penetrates through feathers [Yu, 2014]. Aerodynamics forces due to porosity and their effects on the large flexibility of a

¹Research Assistant, Email: r.rahuma@aerodept.edu.ly

²Professor, Email: aao@aerodept.edu.ly

³Teaching Assistant, Email: abdulhaq.emhemmed@aerodept.edu.ly

wing was examined by Beguin and Breitsamter [Beguin and Breitsamter, 2014]. It was found that the aerodynamic forces can deform the wing surface based on the aerodynamic conditions. Air transitivity of feathers from the ventral to dorsal direction and vice versa was studied by Muller and Patone [Muller and Patone, 1998]. They concluded that both directions have a small difference in air transitivity that is about 10 %. However, significant difference occurs in air transitivity between inner and outer feather vanes. Iosilevskii [Iosilevskii, 2011] analytically studied thin wing membranes segmented into forward solid and aft porous parts, he observed that by keeping the width of the porous segment less than half the wing's chord, the drag can be contained [Iosilevskii, 2013]. The continuously distributed porous surface on airfoil was used by Eppler [Eppler, 1999] to control the flow separation by applying the suction pressure under the porous surface. As reported by few researchers [Zhao and Zhao, 2014; Jiao and Lu, 2015; Chapin and Bnard, 2015], the location and angle of controller were the most important parameters of the controller design in delaying flow separation.

The general goal of this work is to study numerically the effect of the eagle wing porosity on aerodynamics characteristics during gliding flight. Present numerical investigation was performed assuming a two-dimensional incompressible, steady, viscous and low Reynolds number flow. It was also assumed that the bird is gliding. The numerical solver has been verified by testing against the low Reynolds number man made Eppler 193 (E193) airfoil by comparing the obtained numerical results with experimental results for E193 [Selig et al., 1989].

The Eagle airfoil shape was found in references [White, 2008] and then it was drawn to scale using XFLR. After obtaining the coordinates, the airfoil was then meshed. The mesh was a structured C-H mesh with quad cells. The first mesh layer was placed at a distance 1×10^{-6} m from the airfoil surface. This was made to obtain a $y+$ value of approximately 1. Figure 1 shows the mesh for the airfoil at different views.

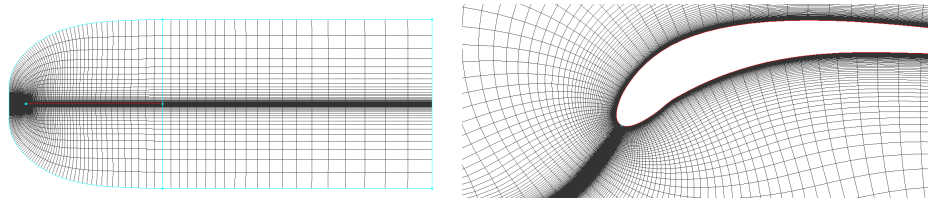


Figure 1: Generated mesh.

All the simulations in this work were run using SU2 CFD code. It is a suite of open source code developed by a number of universities and research institutions led by a team from Stanford University Aerospace Design Laboratory (ADL) [Economon et al., 2016]. The code has solvers for a number of models including Navier-Stokes, RANS, wave equation, heat equations and equations that model solid mechanics. For RANS, SU2 provides a solver for both incompressible and compressible flow.

VALIDATION

The CFD solver was validated against experimental results for the E193 airfoil obtained from Selig et al. [Selig et al., 1989]. The validation case was tested for mesh size, boundary conditions and turbulence model types. $k - \omega SST$ and the SA model have been tested. Validation case provided information about the required boundary conditions, mesh size and appropriate turbulence model.

Figure 2 shows the variation of the lift coefficient, drag coefficient and lift to drag ratio, respectively at different angles of attack for the E193 airfoil. It compares the experimental results and the simulation results obtained using SA and SST model. The comparison of turbulence models is summarized in table 1. By comparing the SA and SST results, it can be concluded that the SST model produces better results for these cases. Therefore the SST models was used for the present work.

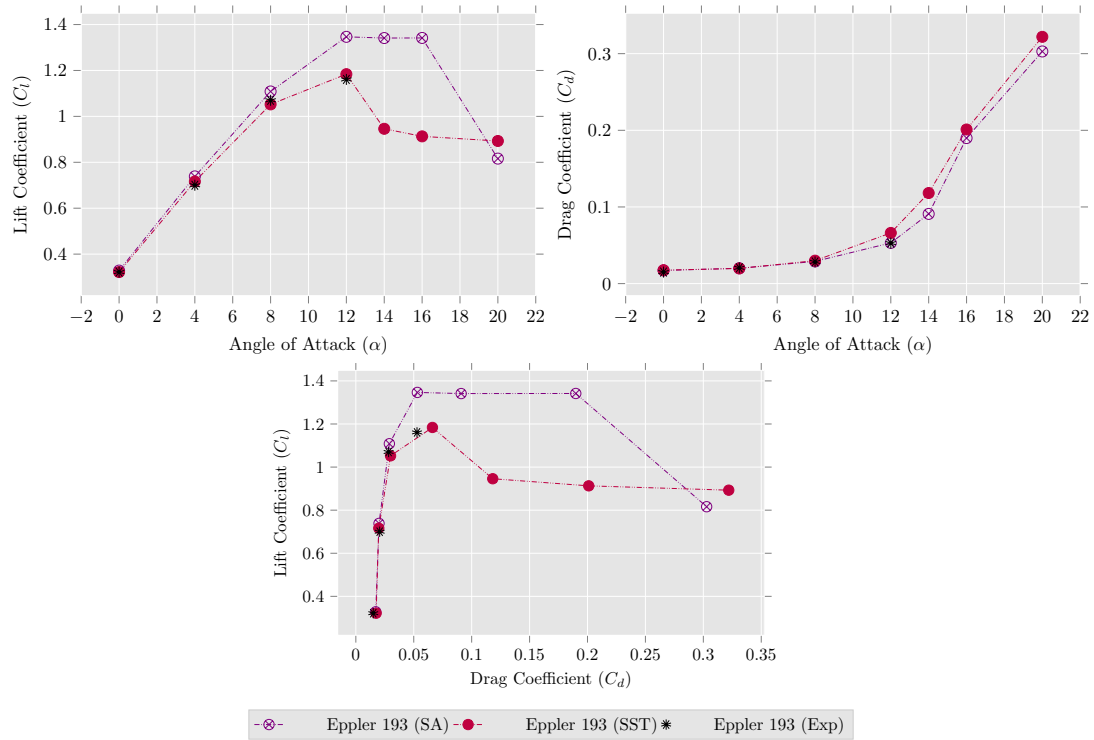


Figure 2: Validation of the lift coefficient, drag coefficient and lift to drag

Table 1: Validation of numerical $C_{l_{max}}$ for E193 [Selig et al., 1989]

Airfoil	α_{stall}	$C_{l_{max}}$	error%
E193 (Experimental)	12°	1.16	-
E193 (SST)	12°	1.18	1.72
E193 (SA)	12°	1.35	16.37

NUMERICAL SETUP

For simulating the eagle airfoil, the porosity was modelled by considering the third of the trailing edge to be a flat plate with holes at every 0.25 cm. A no-slip condition was used for the airfoil surface and far field condition for the domain boundaries. The mesh size was approximately 112 000 cells for non-permeable airfoil and 155 000 cells for permeable airfoil. The Reynolds number (Re) was set to 271 658 for based on the eagle gliding speed. As in the validation case, seven angles of attack were simulated.

All the simulations were run using a Courant-Friedrichs-Lewy (CFL) number of 10 until the solution converged to the desired criteria.

RESULTS & DISCUSSION

Figure 3 shows the variation of C_l , C_d and C_l/C_d for the permeable and non-permeable eagle's airfoil. Table 2 shows the maximum C_l at the stalling angle for the non-permeable and permeable airfoil. Although the permeable airfoil stalls earlier but it is clear from figure 3 that it generates higher lift in comparison to non-permeable at angles of attack lower than the stall angle. The drag coefficient is lower for the permeable airfoil until a certain angle of attack (12°) where drag becomes higher than the non-permeable.

The variation of aerodynamics efficiency C_l/C_d can also be seen in figure 3. The aerodynamic efficiency clearly shows the positive effect of permeability for low angles of attack. Having a permeable section

in the airfoil gives better aerodynamic characteristics when the angle of attack is less than 10° . This is compatible and agrees with observation of other researcher which concluded that “at a transitional phase, where $Re = 40\,000$ and the angle of attack ranged from 0° to 9° , the L/D ratio was higher compared to the same wing without holes” [Geyer et al., 2009]. It seems that after $\alpha = 10^\circ$, turbulent flow has already started or separation has taken place before the permeable part and hence the existence of this permeable part worsens the situation causing less lift to be generated.

From the streamlines figures for the non-permeable cases, those for the permeable and non-permeable eagle’s airfoil are shown in figures4-5. The advantages of the permeable airfoil at low angles of attack is demonstrated by the streamlines. For the non-permeable airfoil small circulation appears on the bottom surface at the leading edge while the streamlines are smooth for the permeable airfoil.

As the angle of attack increases beyond the stall angle, flow separation appears to exist for both airfoils. However, the permeable eagle’s airfoil has more sever separation than the non-permeable eagle’s airfoil.

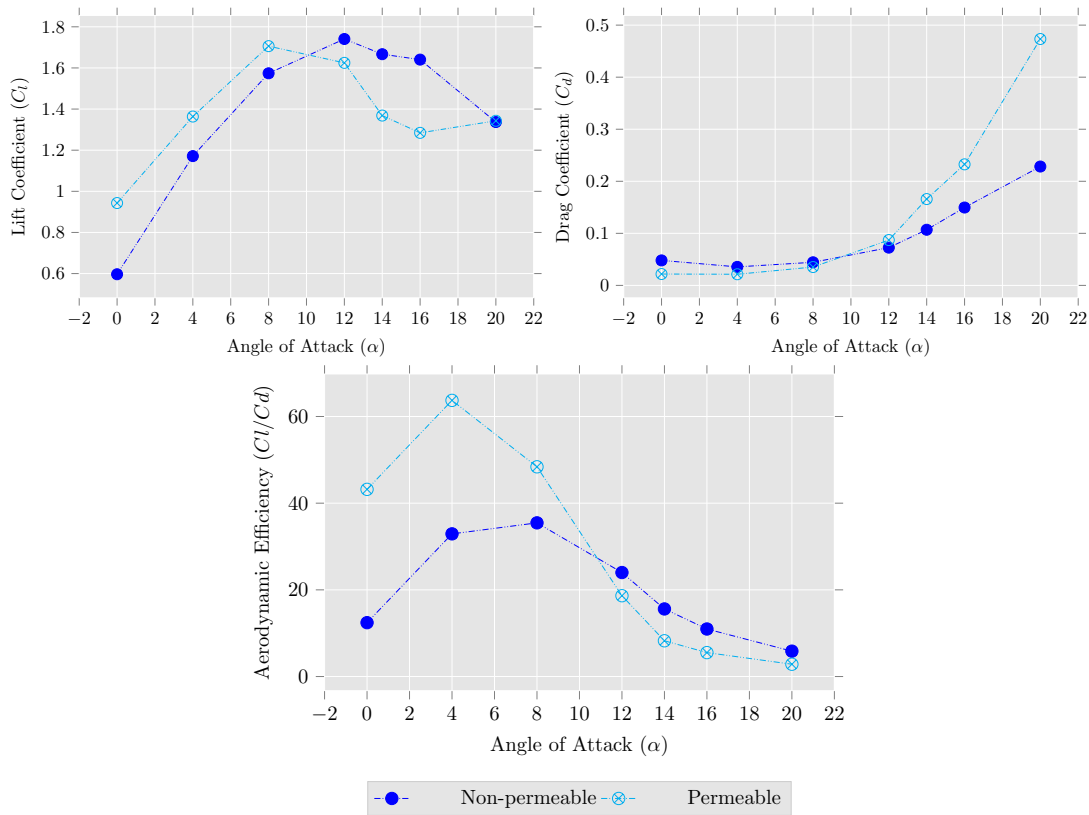


Figure 3: Variation of the lift coefficient, drag coefficient and lift to drag ratio for non-permeable and permeable eagle’s airfoil

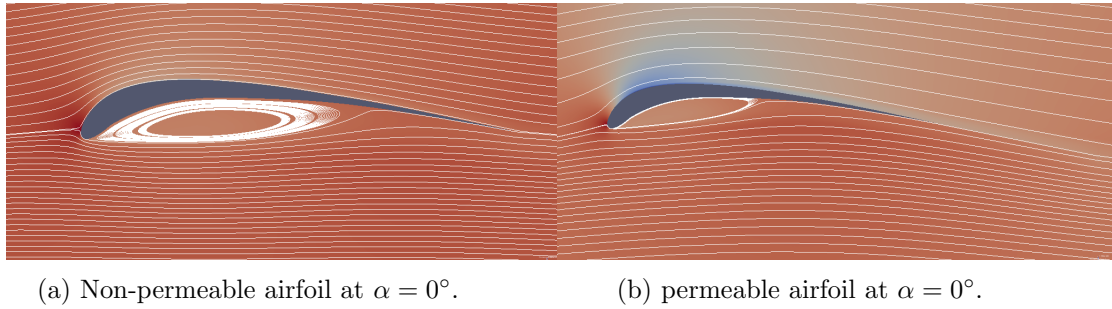


Figure 4: Distribution of stream lines at zero angle of attack for permeable and non-permeable eagles airfoil.

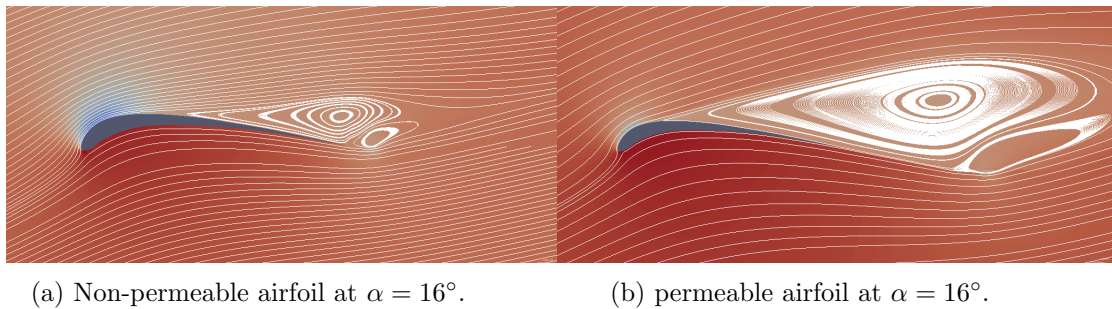


Figure 5: Distribution of stream lines at high angle of attack for permeable and non-permeable eagles airfoil.

Table 2: Value of lift coefficient for non-permeable and permeable eagle's airfoil

Airfoil	α_{stall}	$C_{l_{max}}$
Non-permeable airfoil	12°	1.74
Permeable airfoil	8°	1.71

CONCLUSION

The aim of this study was to investigate the aerodynamic performance of eagle's airfoil under permeable and non-permeable conditions, comparison was made between the two cases. Reasonable agreement has been made between the obtained simulation results for Eppler 193 using the SST turbulence model and the experimental data. This demonstrated the validity of the used flow solution algorithm.

Finally, making the eagle's airfoil permeable improved the efficiency for angles of attack less than 10° . But it had adverse effects for higher angles of attack.

References

- Beguin, B. and Breitsamter, C. (2014). Effects of membrane pre-stress on the aerodynamic characteristics of an elasto-flexible morphing wing. *Aero Sci Tech*, pages 138–150.
- Chapin, V. and Bnard, E. (2015). Active control of a stalled airfoil through steady or unsteady actuation jets. *Journal of Fluids Engineering*, 137.
- Economon, T. D., Palacios, F., Copeland, S. R., Lukaczyk, T. W., and Alonso, J. J. (2016). Su2: An open-source suite for multiphysics simulation and design. *AIAA Journal*, 54:828–846.
- Eppler, R. (1999). Airfoils with boundary layer suction, design and off-design cases. *Aerospace Science and Technology*, 3:403–415.
- Geyer, T., Sarradj, E., and Fritzsche, C. (2009). Porous airfoils: Noise reduction and boundary layer effects. *30th AIAA Aeroacoustics Conference*.
- Iosilevskii, G. (2011). Aerodynamics of permeable membrane wings. *European Journal of Mechanics-B/Fluids*, 30:534–542.
- Iosilevskii, G. (2013). Aerodynamics of permeable membrane wings. part 2. *European Journal of Mechanics-B/Fluids*, 39:32–41.
- Jiao, Y. and Lu, Y. (2015). Parameter optimization research on lift-enhancing of multi-element airfoil using air-blowing. *Procedia Engineering*, 99:73–81.
- Muller, W. and Patone, G. (1998). Air transmissivity of feathers. *Journal of Experimental Biology*, pages 2591–2599.
- Selig, M. S., Donovan, J. F., and Fraser, D. B. (1989). *Airfoils at Low Speeds*. H.A. Stokely.
- White, F. M. (2008). *Fluid Mechanics*. McGraw Hill, 6 edition.
- Yu, H.-T. (2014). *Unsteady aerodynamics of pitching flat plate wings*. PhD thesis, The University of Michigan.
- Zhao, G. and Zhao, Q. (2014). Parametric analyses for synthetic jet control on separation and stall over rotor airfoil. *Chinese Journal of Aeronautics*, 27:1051–1061.